Position Control of a DC Servo Multi-motor for Lower-Limb Exoskeletons

Rina Ristiana
Research Center of Transportation Technology, National Research and Innovation agency, West Java, Indonesia
rina008@brin.go.id
0000-0002-7842-1126

Rina Mardiati
Department of Electrical Engineering, UIN Sunan Gunung Djati Bandung, West Java, Indonesia
r_mardiati@uinsgd.ac.id
0000-0002-3949-7830

Dwi Esti Kusumandari
Research Center of Smart Mechatronic, National Research and Innovation agency, West Java, Indonesia
dwie002@brin.go.id
0000-0002-9050-6616

Artha Ivonita Simbolon
Research Center of Smart Mechatronic, National Research and Innovation agency, West Java, Indonesia
arth001@brin.go.id
0000-0002-5303-6547

M. Faizal Amri
Research Center of Smart Mechatronic, National Research and Innovation agency, West Java, Indonesia
mfai001@brin.go.id
0000-0002-6390-2883

Jony Winaryo Wibowo
Research Center of Smart Mechatronic, National Research and Innovation agency, West Java, Indonesia
jony001@brin.go.id
0000-0001-6459-3835

2022 8th International Conference on Wireless and Telematics (ICWT) | 978-1-6654-5122-2/22/$31.00 ©2022 IEEE | DOI: 10.1109/ICWT55831.2022.9935372

***Abstract*— The angular position control of DC servo multi-motor using PID control has been proposed. The PID controller tuning is applied to the Ziegler-Nichols (ZN) method. The angular position control of the DC motor is built in the mixed (cascade) system consisting of six electric motors to drive the joint movement of the lower-limb exoskeleton (hip, knees, and ankle). The PID control design is implemented in the lower-limb exoskeleton and experimental setup and simulation are carried out to obtain proper proportional, integral, and derivative gains. Based on these gains, the PID controller gives a good response, without overshoot, fixed settling time, and is precise to get the desired angle.**

Keywords—Position Control, DC Servo Motor, PID Controller, the Ziegler-Nichols Method, Lower-limb Exoskeleton.

I. INTRODUCTION

At the time when the humans are active or move, strong and durable muscles are needed, but the human muscles have a limit of fatigue when doing regular and repetitive activities. To help overcome this fatigue problem, it is recommended to use an external device, namely an exoskeleton. The exoskeleton is a system that can be used to help the humans support and protect their body parts. This device has been widely used, one of which is as a medical therapy or rehabilitation tool that has been used to help patients who have lost the ability to walk due to spinal cord injury, stroke, trauma, and so on. The rehabilitation exoskeletons can improve the quality of exercise during rehabilitation and can speed up the recovery process.

The application of the exoskeleton to the human body generally consists of: throughout the human body, the upper part of the human body (torso and arms), and the lower part of the human body (the waist down). All parts of the human body simultaneously play a specific function in supporting the movement of walking. However, the lower-limbs play an important role compared to other parts of the body, because the lower-limb supports the body weight, helping to move by generating torque when walking. Therefore, the discussion focuses on the lower-limb exoskeleton.

The lower-limb exoskeleton discusses the movement of joints and the types of actuators during movement. The joints in the lower-limb exoskeleton of the human body are the hips, knees, and ankles. Each joint has a different ability to move or is called the degree of freedom (DOF). The exoskeletons have multiple actuators to drive a combination of joints. One of the medical exoskeletons applied the DC servo motor as the actuator for the joint's motion source. The combination of the actuator namely the DC servo multi-motor drives the hips, knees, and ankles. The DC servo motor is designed with a closed loop feedback control system which can be adjusted to determine and ensure the angular position of the motor shaft.

Several studies on controlling the motor angle position based on modification of the order system, as described in [1] developed the differential equations of DC motor with reduction order. This gives rise to nonlinearities that may lead to instability effect and may not be adopted for high power tasks. In [2] designed a fractional order PI and PD controller for speed and position control based on time domain specification. The result is the fractional order controllers outperform the classical controllers. In [3] present multiple controller design for speed and position control DC motor. The control method is proportional, PID, lag-led, and full-state feedback controllers. The PID controller design meets the requirements with the least error and is thus chosen as final design.

Furthermore, position control can also be carried out based on the implementation of different algorithms in applications such as: in [4] compared the dc motor positioning control of PID algorithm in Matlab and Labview with seen transient response and a state space controller. Labview with suitable acquisition is used for experimental assessment. Matlab is used calculation and control system simulations. The result is the state space controller is modelled by using Matlab more accuracy than Labview. In [5] The PID controller was implemented in LabVIEW software which sends the control signal to the real time DC motor through the Arduino board and was developed to show the output response of motor position versus time to easily observe the performance of the system. The results showed that the designed controller had good performance characteristics where the desired position of the motor was maintained.

There are also angular position controls with generated PWM and specify robustness, such as in [6] present to get the precision of angular position control of DC motor using PID control. The PID controller tuning methods with generated the PWM output. But, it has a few errors when the orientation of changes angle because it are not fast to reach the desired position. Therefore, friction compensation according to the velocity effect is considered. After compensating the friction effect, the PID output results were very precise to get the desired angle. In [7] presents a synthesis method of a low-order H∞ robust controller to control the position of a DC motor. The synthesis employed Differential Evolution optimization to find a controller that guarantees robust stability performance and robust stability against system perturbation. However, the proposed controller gives a better response in terms of overshoot and response time.

The paper proposed the angular position control with implemented the PID controller tuning using the Ziegler-Nichols (ZN) method. The angular position control of the DC motor is built in the mixed (cascade) system consisting of six electric motors to drive joint movement of the lower-limb exoskeleton (hip, knees, and ankle). Furthermore, experimental setup and simulation are carried out to get the right proportional, integral, and derivative gains. It is expected that the PID controller gives good response, without overshoot, fixed settling time, and precise to get the desired angle.

The rest of this paper is organized as follows; Section II describes the description system. It is followed by the position control of a multi-motor DC servo design in Section III. experimental setup and discussion are then presented in Section IV. Section V finalizes the paper with the main conclusion.

II. The Description System

Generally, the lower-limb therapies use to practice passive gaits where the exoskeleton guides limb movements to improve active practice systems. The joint movement aims to achieve the optimal effect from a therapeutic and functional point of view which achieved effective muscle strengthening. The challenge of the active practice system is the coordination of movements between the exoskeleton and the user.

The exoskeleton discusses the joints movement and the types of actuators. The actuator exoskeleton is classified into two types, namely electric motor and pneumatic artificial muscle (PAM). Generally, exoskeletons use motors to move their joints, and the exoskeleton framework is the same as that of humans. Usually, exoskeleton designs are based on anthropometric factors of the human body [8]. The exoskeleton illustrating the lower human body is embodied in the lower-limb exoskeleton. In the design of the joint movement, a control scheme is needed that requires a high level of safety and accuracy.

Based on anthropometry, the motion range of the human joint must be determined by the comfort angle of the joint so as not to cause pain and even danger to the user. The comfort angles are given in Table I. These comfort angles are used to design the joint range of the exoskeleton.

TABLE I. COMFORT ANGLES OF LOWER-LIMB JOINTS [9], [8]

Joint	Movement	Range (^{0})
Hip	Hyperextension Flexion	0-45 0-130
Knee	Flexion	0-135
Ankle	Dorsiflexion Plantarflexion	0-20 0-40

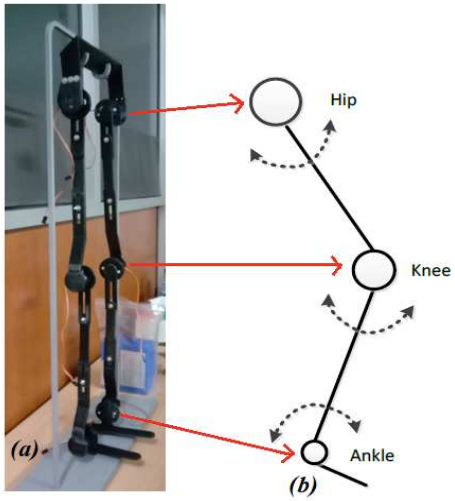

Fig.1. 3D Lower-limb Exoskeleton

The design of the joint is to align the anatomical axis of rotation. The lower-limb exoskeleton used has 6-DOF with a scale of 10:1 from the size of the human body as shown in Fig. 1a. The link exoskeleton is made of polymathic-acid filament made by a 3D printer. The hip and knees exoskeleton is an active flexion/extension joint that serves to increase lower-limb strength and a DC motor actuator is applied directly to the joint. The ankles are a passive flexion/extension joint. The flexion is the positive direction and the extension is the negative direction of the sagittal plane (the plane that divides the human body into right and left halves). The relationship between the hips, knees, and ankle joint are illustrated in Fig. 1b. The connection customized with the link.

The cycle of the human walking gait can be represented in Fig. 2. The gait cycle starts from right heel contact and ends in the same condition. The cycle determines the movement of the exoskeleton [10]. The relationship between gait cycle and hip angle that needs to be considered includes the walking gait or run gait, walking on a flat surface or incline, and the user's weight is thin or fat [11]. The movement relationship for each joint between the hip and ankle occurred abduction (movement of pulling away from the middle of the body) vs. adduction (movement of pushing toward the center of the body) and eversion (movement away from the midline of the body) vs. inversion (movement towards the midline of the body) [12].

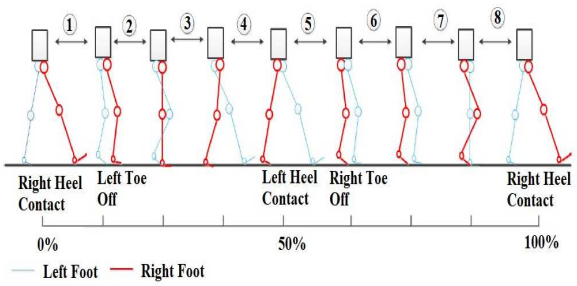

No	1	2	3	4	5	6	7	8
Right Leg	Heel strike	Loading response	Mid stance	Terminal stance	Pre swing	Toe off	Mid Swing	Terminal Swing
Left Leg	Pre swing	Toe off	Mid swing	Terminal swing	Heel strike	Loading response	Mid stance	Terminal stance

Fig. 2. The human walking gaits [10].

Exoskeleton safety factors include mechanical, electrical and software design. Mechanical design uses physical characteristics to prevent segments at joints. The electrical part is as a regulator of motor movement. While the software to monitor the integrity of power transmission and limiting motor current and torque. When the motor moves close to the threshold limit, a brake command is sent, the software determines the maximum and minimum range of each joint.

The actuator of the exoskeleton is a DC servo motor. The servo motor is a rotary device or actuator designed with a closed loop feedback control system. The servo motor can be set-up or adjusted to determine and ensure the angular position of the motor shaft. Servo motor is a device consisting of a DC motor, a series of gears, a control circuit and a potentiometer. A series of gears attached to the DC motor shaft will slow down the rotation of the shaft and increase the torque of the motor, while the potentiometer functions to change the resistance when the motor rotates and as a determinant of the angular position. The use of a closed loop system on a servo motor is useful for controlling the movement and final position of the servo motor shaft.

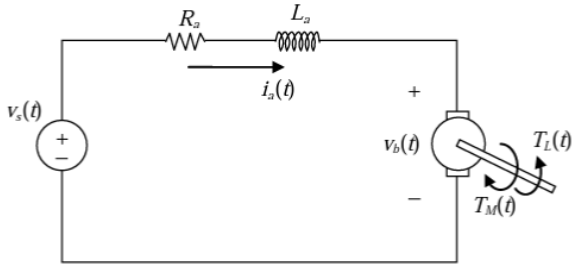

Consider a standard DC motor model as depicted in Fig 3. The electrical differential equation governing the dynamics are [13]

$$\frac{di_a(t)}{dt} = -\frac{R_a}{L_a} i_a(t) - \frac{k_e}{L_a}\omega_m(t) + \frac{1}{L_a} V_s(t) \quad (1)$$

with i_a is the armature current, R_a is the armature resistance, L_a is the winding leakage inductance, V_b is the back emf voltage ($V_b(t) = k_e\omega_m(t)$), k_e is the back emf constant, ω_m is the angular motor speed, and V_s is the motor voltage source. The motor generates a torque (T_m) proportional to the armature current, given as

$$T_m(t) = k_t i_a(t) \quad (2)$$

where k_t is the torque constant. Besides, if the DC motor is used to drive an external torque (T_L) of payload and (2) then its mechanical behavior is described as

$$\frac{d\omega_m(t)}{dt} = \frac{k_t}{J_m} i_a(t) - \frac{B_m}{J_m}\omega_m(t) + \frac{k_t}{J_m} i_a(t) - T_L(t) \quad (3)$$

with J_m is the rotor moment of inertia and B_m is the frictional coefficient.

The goal of control is drive the DC motor to a desired angle, then the output should be set as the angular position $\theta_m(t) = \int_0^t \omega_m(\tau)\, d\tau$. The angular position changes into the differential form as below:

$$\frac{d\theta_m(t)}{dt} = \omega_m(t) \quad (4)$$

Referred to (1), (3), and (4),without any payload, choosing the state variable as $x_s(t) = [x_1(t) \quad x_2(t) \quad x_3(t)]^T$, with $x_1(t) = i_a(t)$, $x_2(t) = \omega_m(t)$, and $x_3(t) = \theta_m(t)$. The input vector is $u_s(t) = V_s(t)$. The state space (5) and the output equation (6) is given as

$$\dot{x}_s(t) = A_s x_s(t) + B_s u_s(t) \quad (5)$$
$$y_s(t) = x_3(t) \quad (6)$$

with $A_s \in \mathcal{R}^{n\times n}$, $B_s \in \mathcal{R}^{m\times n}$, and $C_s \in \mathcal{R}^{n\times m}$, the system matrices are

$$A_s = \begin{bmatrix} -\frac{R_a}{L_a} & -\frac{k_e}{L_a} & 0 \\ \frac{k_t}{J_m} & -\frac{B_m}{J_m} & 0 \\ 0 & 1 & 0 \end{bmatrix}, B_s = \begin{bmatrix} \frac{1}{L_a} \\ 0 \\ 0 \end{bmatrix}, \text{and } C_s = [0 \quad 0 \quad 1].$$

III. The Position Control of The Multi-Motor Design

The lower limb exoskeleton in Fig. 1a has 6 DOF of joint movement, namely the hip (right and left), knees (right and left), and ankle (right and left). Each joint movement of the exoskeleton is applied the DC servo motor as the actuator for the joint's motion source. Thus, the exoskeleton has six DC servo motors or called multi-motors. Each DC servo motor is adjusted to determine and ensure the angular position is in accordance with the cycle of the human walking gait. Each motor has the same system model as described in (6) and (7), the difference is the reference value for each motor. It is adjusted to the angular position of the dc motor functioned as hips, knees or ankles.

In this paper applied the standard proportional-integral-derivative (PID) control for setting the angular position. The design of the PID controller is done by tuning the gain K_p, K_i, and K_d. The tuning is done in order to obtain a good output response system, which has a steady state error, the output response reaches a steady state with the correct steady state and transient time. The PID controller is described by the following equation;

$$u_c(t) = K_p e_\theta(t) + K_i \int_0^t e_\theta(\tau)\, d\tau + K_d \frac{de_\theta}{dt} \quad (7)$$

With K_p, K_i, and K_d are prpoportional, integral, and derivative gains of the PID controller, respectively. $e_\theta(t)$ is error state which determined from the desire output system $\theta_m(t)$ and the input reference $\theta_{m,ref}(t)$, or can be written $\theta_\omega(t) = \theta_{m,ref}(t) - \theta_m(t)$.

Typical steps for designing a PID controller are determine the characteristics of the system need improved, use K_p to decrease the rise time, use K_i to eliminate the steady-state error, and use K_d to reduce the overshoot and settling time. A popular method for tuning PID controller is the Ziegler-Nichols (ZN) method. This method starts by zeroing the integral and differential gains, and then raising the proportional gain until the system is unstable.

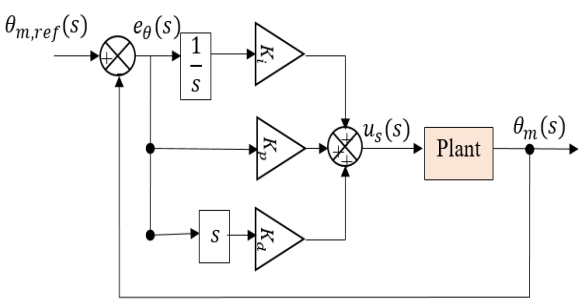

Fig. 4. PID controller design.

The ZN method conducted numerous experiments and proposed rules for determining values of K_p, K_i, and K_d based on the transient step response of the plant. The value of K_p at the point instability or increased (from zero) until it reaches the ultimate gain (K_u) which the output of the control loop has stable and consistent oscillations. The frequency of oscillation is f_o. The method then backs off the proportional gain predetermined amount and sets the integral and differential gains as a function of f_o. The P, I, and D gains depending on the type of controller used and behavior desired as below [14] and the PID controller design scheme as shown in Fig. 4.

$$K_p = 0.6 \times K_u \quad (8)$$

$$K_i = 2.0 \times f_o \quad (9)$$

$$K_d = 0.125/f_o \quad (10)$$

IV. Experimental Setup and Discussion

An experimental setup is a characteristic test on the DC servo multi-motor of the lower limb exoskeleton. The experimental setup can be seen in Fig. 5, there are the lower-limb exoskeleton scale 10:1 from the human body. The links are made of polymathic-acid filament made with a 3D printer. Each joint is connected to a DC servo motor actuator as many as six joints, namely hips (right and left), knees (right and left), and ankles (right and left). Each DC servo motor is connected to a PCA9685 module which helps when the PWM output pin is insufficient and can control multiple servo motors simultaneously [15]. As the unit processing module used an Arduino Nano microcontroller based on ATmega328 which all pins operate at a voltage of 5V and can provide/receive a maximum current of 40mA, and have an internal pull-up resistor of 50KOhm. The control module is equipped with automatic and manual modes for the reference signal. The automatic mode is set by providing a reference signal in the programming, while the manual mode is by using a potentiometer. The potentiometer can be set according to the conditions and the cycle gait, which be replaced with an electromyography (EMG) or electroencephalography (EEG) sensor.

DC servo motors used are SG90 motor for ankles (right and left) and SPT543LV motor for knees (right and left), and hip (right and left). The position control can be done by providing a pulse wide modulation (PWM) signal so that the angular position of the motor is obtained from the motor shaft. In this experiment, the initial motor shaft is determined at an angle of 90 degrees, this is done to get the motor rotational balance and make programming easier. With the initial angle position at 90 degrees, the motor can rotate CW by 0 degrees and CCW by 180 degrees. The reference signal determined for the joint movement according to the cycles of the human walking gait, as can be seen in Table II. For example, if the angle position in the table is 30, which means 90+30, it means that the reference value is 120 degrees (CW 30 degrees), or -20 means 90-20 means a reference value of 70 degrees (CCW 20 degrees).

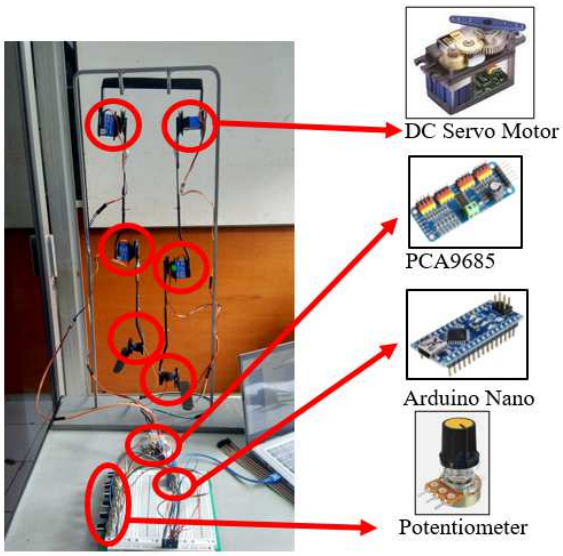

Fig. 5. Experimental setup.

TABLE II. The Cycle of The Walking Gaits

No	Hip		Knees		Ankles	
	Right	Left	Right	Left	Right	Left
1	30	-5	65	-20	15	0
2	8	8	20	20	0	-5
3	0	8	0	30	0	-15
4	-8	8	-30	20	-5	5
5	30	-5	65	-20	15	0
6	8	8	20	20	0	-5
7	0	8	0	30	0	-15
8	30	-5	65	-20	15	0

As seen in Fig. 5, the exoskeleton drive module consists of the Arduino Nano microcontroller, PCA9685, and potentiometer. The schematic diagram of the drive module can be seen in Fig. 6, Arduino pin A4 is connected to pin SDA on PCA9685, Arduino Pin A5 is connected to pin SCL on PCA9685. Each pin 2 of the potentiometer is connected to pins A0, A1, A2, A3, A6, and A7 on the Arduino. Each pin 2 DC servo motor is connected to pins Led0 to Led5 on PCA9685. For the purposes of simulation and test setup, DC servo motor parameters are used as shown in Table III.

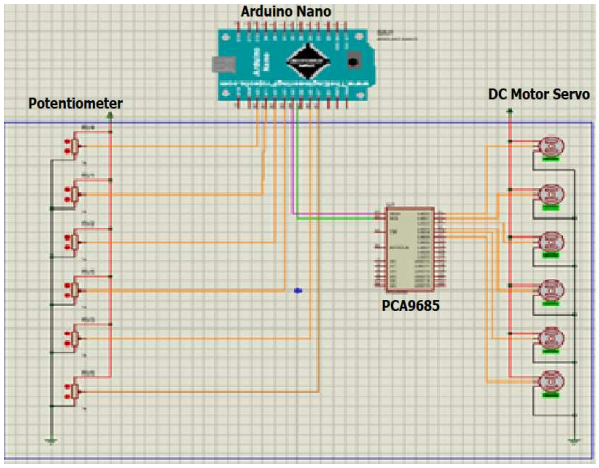

Fig. 6. Diagram block drive module.

TABLE III. Motor Parameters

Description	Symbol	Value	Unit
Armature Resistance	R_a	0.5	Ohm
Armature Inductance	L_a	1.5	mH
Moment Inertia	J_m	2.5×10^{-4}	Nm/(rad/s)
Coefficient Torque	k_t	0.05	Nm/A
Coefficient Back emf	k_e	0.05	V/(rad/s)
Coefficient Friction	B_m	1.0×10^{-4}	Nm/(rad/s)

Referred to (5), and (6), the plant (system) is changed from the state space to the transfer function. Furthermore, the DC servo motor parameter values are given in Table 2, so that the transfer function system is obtained in the following numerical form:

$$TF_s(s) = \frac{133334}{s(s+21.80)(s+311.93)} \quad (11)$$

Based on (11) given the pole at $s_1 = 0$, $s_2 = -21.80$, and $s_3 = -311.93$, which implies the pole at s_3 can be omitted since it is much faster than the pole at s_2. In other words, the transfer function can be approximated by a second order transfer function.

The tuning of the PID controller according to the ZN method which given the value of the ultimate gain (K_u) is 4.8, and The frequency of oscillation (f_o) is 311Hz, then it given the value of the K_p, K_i, and K_d in two mode. The first at $K_p = 1.7$, $K_i = 120$, and $K_d = 0.0002$, and the second $K_p = 2.9$, $K_i = 622$, and $K_d = 0.0004$.

Both modes of P, I, and D gains are implemented in the multi-motor model. For simulation purposes, the reference value of the angle position is 25 degrees for each motor. Based on the simulation results shown in Fig. 7, it is illustrated that a good response is PID controller mode-1, which has a settling time of 0.3 seconds, without over/undershoot, and can reach steady state well, while PID controller mode-2 has settling time 0.6 seconds (slower 0.3 seconds than mode-1), there is an undershoot, and does not reach steady state properly. Henceforth, the PID gains mode-1 value is used in the multi-motor system.

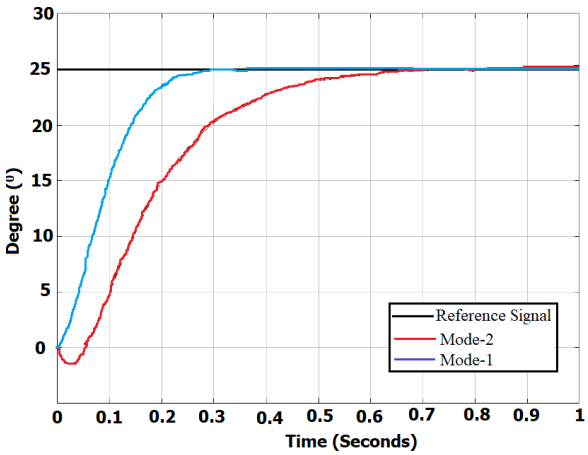

Fig. 7. PID controller response with ZN method.

The experimental results show the feasibility of the controller developed in (7) to (10). The designed controller exploits kinematic and angular position feedback for each joint. In this experiment only analyzed the hip (right and left) and knees (right and left) responses, because the ankle joint (right and left) does not show a significant change. The exoskeleton stiffness that affects the joint kinematics, and the intensity of stimulation at the hips (right and left) and knees (right and left). Thus the electric motor can affect the respective lower-limb kinematics as illustrated in Fig. 8. The developed controller achieves a repeatable and consistent kinematic joint trajectory as a gait function with a standard deviation of the joint angle of about 5.85 degrees (right knee), 5.03 degrees (right hip), 8.57 degrees (left knee), and 5.88 (left hip).

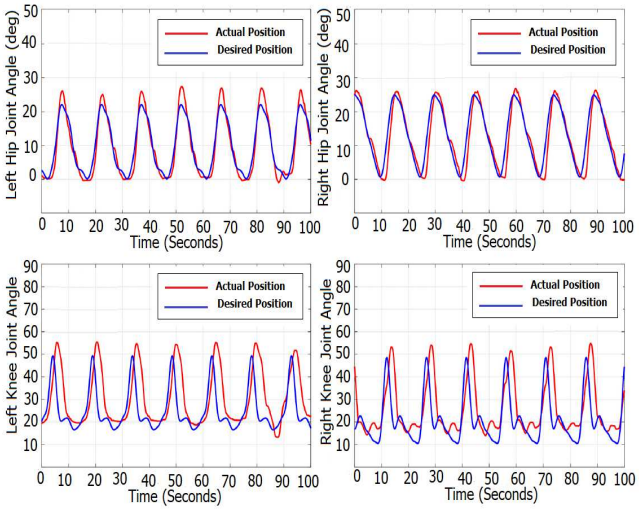

Fig. 8. Kinematics tracking performance.

From Fig. 8, can be shown a kinematics tracking performance when the cycle of the human walking gaits. The eighth of the gait cycle is performed over a period of 100 seconds at the same walking speed. Each joint angle can be calculated for each movement. The hips have an angle limit of about 0 to 28 degrees, while knees have an angle limit of 8 to 55 degrees for a walking speed of about 2 m/sec.

For the kinematics joint trajectory of the gait cycle can be shown in Fig. 9, it presents how the lower-limb movement (right or left) simultaneously when the walking cycle. The gait cycle for the right hip and the left hip have the opposite graph, as well as for the right and left knee. Referred to the experimental setup, it can be concluded that the multi-motor position control using the PID controller with tuning based on the ZN method can be applied, and the PID controller gives a good response, without overshoot, fixed settling time, and precise to get the desired angle.

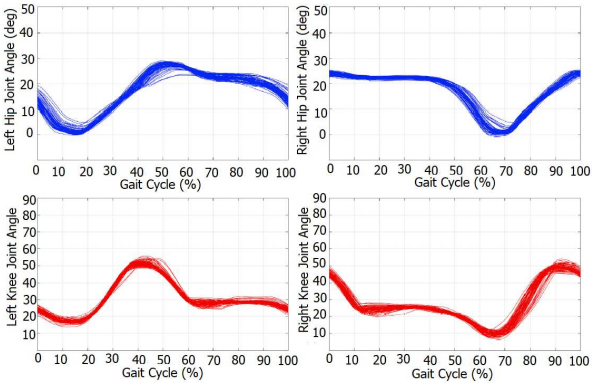

Fig. 9. Kinematics Joint Trajectory

V. Conclusion

The angular position control using the PID controller is proposed. The PID tuning is applied the ZN method. The value of the K_p, K_i, and K_d gains is given in two mode and implemented into the multi-motor model. The PID controller mode-1 has a good response, without over/undershoot, reached the steady state well, and settling time is faster at 0.3 seconds from the other. The PID controller mode-1 applied for the angular position control of the exoskeleton with the cycle of the human walking gaits. The result is precise to get the desired angle.

REFERENCES

[1]. J. Goncalves and M. Marques, "DC Motor Control Position," Universidade do Minho, 2013.

[2]. C. Copot, C. I. Muresan and R. De Keyser, "Speed and Position Control of a DC Motor using Fractional Order PI-PD Control," 3rd International Conference on Fractional Signals and Systems, Ghent, Belgium, 2013.

[3]. R. Awar, Y. K. Al Ali and Y. Al Jrab, "Speed and Postition Control of a DC Motor," American University of Beirut, Beirut, Lebanon, 2009

[4]. N. Bacac, V. Slukic, M. Puskaric, B. Stih, E. Kamenar and S. Zelenika, "Comparison of Different DC Motor Positioning Control Algorithm," in *37th International Convention on Information and Communication Technology, Electronics and Microelectronics (MIPRO)*, 2014.

[5]. M. Saad, A. H. Amhedb and M. Al Sharqawi, "Real TIme DC Motor Position Control Using PIS Controller in Labview," *Journal of Robotics and Control,* vol. 2, no. 5, pp. 342-348, 2021.

[6]. M. Maung, L. Maung and C. M. Nwe, "DC Motor Angular Position Control using PID Controller with Friction Componsation," *International JOurnal of Scientific and Research Publication,* vol. 8, no. 11, pp. 149-155, 2018.

[7]. P. Sutyasadi, "An Improved DC Motor Position Control using Differential Evolution Based Structure Specified H∞ Robust Controller," *Jurnal Ilmiah Teknik Elektro Komputer dan Informatika,* vol. 7, no. 2, pp. 347-357, 2021.

[8]. P. Leon, G. Munoz and A. Chaurand, "Dimensiones on Antropometricas de Poblacion Latinoamericana," Universidad de Guadalajara, Mexico, 2012.

[9]. R. Contini, "Body Segment Parameters," *Artif Limb,* vol. 16, no. Part II, pp. 1-19, 1972.

[10]. E. Davis, Gait Joint Structure and Function: A Comprehensive Analysis, MCGraw-Hill, 2019.

[11]. J. Moore, S. Hnat and V. D. Bogert, "An Elaborate Data Set on Human Gait and The Effect of Mechanical Pertubations," *PeerJ,* vol. 3, no. 918, pp. 1-20, 2015.

[12]. A. Voloshina and D. Ferris, "Biomechanics and Energetics of Running on Uneven Terrain," *Journal of Biology,* vol. 218, pp. 711-719, 2015.

[13]. R. Ristiana, A. Syaichu-Rohman, C. Machbub, A. Purwadi and E. Rijanto, "A New Approach of EV Modeling and its Control Application to Reduce Energy Consumption," *IEEE Access,* vol. 7, pp. 141209-141225, 2019.

[14]. G. Ellis, Control System Design Guide Using Your COmputer to Understand and Diagnose Feedback Controllers, FOurth Edition, Butterworth-Heinemann: Elsevier Inc., 2012.

[15]. A. M. Shojaei, "Motors & Drivers," 28 Maret 2022. [Online]. Available: https://electropeak.com/learn/interfacing-pca9685-16-channel-12-bit-pwm-servo-driver-with-arduino/.